Physica Scripta. Vol. T70, 79–87, 1997

Linear Superpositions of States in Radiative Processes

C. Cohen-Tannoudji

Collège de France et Laboratoire Kastler Brossel,* de l'Ecole Normale Supérieure, 24 rue Lhomond, 75231 Paris Cedex 05, France

Received February 27, 1996; accepted May 15, 1996

Abstract

When an atom, in a linear superposition of states, absorbs or emits light, interference can occur between two different absorption or emission amplitudes, giving rise to observable physical effects, such as level crossing resonances, quantum beats, and dark states. Early experimental demonstrations of effects of this kind, using an optical detection of the atomic internal state, are briefly reviewed. In fact, such interference effects are still playing a fundamental role in modern developments, such as laser cooling and trapping. We present in this paper a few examples of such applications, including the mechanical Hanle effect, velocity selective resonances for an atom moving in a standing wave and subrecoil laser cooling by Velocity Selective Coherent Population Trapping (VSCPT).

1. Introduction

One of the most fascinating features of quantum mechanics is the fact that quantum amplitudes interfere. Several examples of such interferences can be found in radiative processes. Consider for example a photon scattering process $\boldsymbol{k} \rightarrow \boldsymbol{k}'$ by an atom in a magnetic field $\boldsymbol{B}$, $\boldsymbol{k}$ and $\boldsymbol{k}'$ being the wave vectors of the incident and scattered photon, respectively (Fig. 1a). We suppose that the atom has two Zeeman sublevels e_1 and e_2 which cross for a certain value B_0 of the field (Fig. 1b). Near resonance, there are two important paths which contribute to the scattering amplitude and which are represented by the two diagrams of Fig. 2. The atom in g absorbs the incident photon and goes into e_1 (Fig. 2a) or e_2 (Fig. 2b), and then emits the scattered photon $\boldsymbol{k}'$ while returning to g. The two paths have the same initial and final states, but different intermediate states. Therefore, the two corresponding amplitudes interfere. The amplitude of the process of Fig. 2a becomes large when the energy splitting $E_{e_1} - E_g$ between e_1 and g is equal to the energy $\hbar\omega = \hbar ck$ of the incident photon, within $\hbar\Gamma$ (Γ being the natural width of the excited state). Similarly the amplitude of the process of Fig. 2b becomes large when $E_{e_2} - E_g = \hbar\omega$ (within $\hbar\Gamma$). It follows that the two amplitudes can both become large only if E_{e_1} and E_{e_2} differ by less than $\hbar\Gamma$, i.e. near the crossing point $B = B_0$. It is then easy to understand why the interference term between the two scattering amplitudes associated with the processes of Fig. 2 gives rise to resonant variations of the scattered light when B is scanned around B_0, in an interval determined by $|E_{e_1} - E_{e_2}| \leqslant \hbar\Gamma$. Such a resonance, which is Doppler free, can be observed around $B_0 = 0$, since all Zeeman sublevels cross in zero field. This is the well known Hanle effect [1]. Two Zeeman sublevels belonging to two different hyperfine levels can also cross for a non zero value of B_0. The corresponding resonant variations of the scattered light around B_0 are known as the Franken effect [2].

Another way of interpreting the previous effects is to consider that the absorption of the incident photon prepares the atom in a linear superposition of the two excited Zeeman sublevels e_1 and e_2. In other words, the density matrix σ which describes the excited atomic state has not only diagonal elements $\sigma_{11} = \langle e_1|\sigma|e_1\rangle$ and $\sigma_{22} = \langle e_2|\sigma|e_2\rangle$, which represent the populations of e_1 and e_2, but also off-diagonal elements $\sigma_{12} = \langle e_1|\sigma|e_2\rangle = \sigma_{21}^*$. When such "Zeeman coherences" exist, there is some anisotropy in the atomic excited state in the plane perpendicular to $\boldsymbol{B}$, described by a transverse orientation ($\langle J_+\rangle \neq 0$, where $J_+ = J_x + iJ_y$, $\boldsymbol{J}$ being the angular momentum and the $z-$axis being taken along $\boldsymbol{B}$), or a transverse alignment ($\langle J_z J_+\rangle \neq 0$ or $\langle J_+^2\rangle \neq 0$). The intensity of the light emitted by the atom in a given direction generally depends

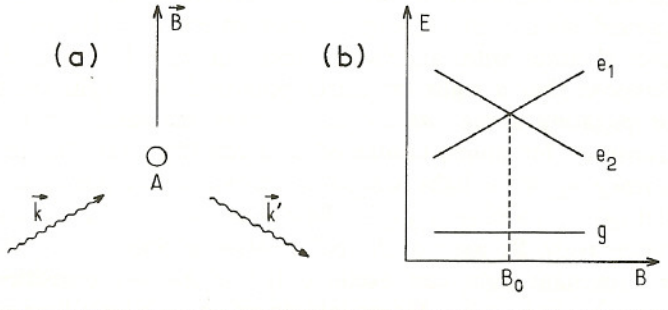

Fig. 1. (a) An incident photon, with wave vector $\boldsymbol{k}$ is scattered by an atom put in a magnetic field $\boldsymbol{B}$; $\boldsymbol{k}'$ is the wave vector of the scattered photon. (b) When the amplitude B of the magnetic field is scanned, two excited Zeeman sublevels of the atom e_1 and e_2 cross for a certain value B_0 of B. We suppose here that the atom has a single ground state Zeeman sublevel g.

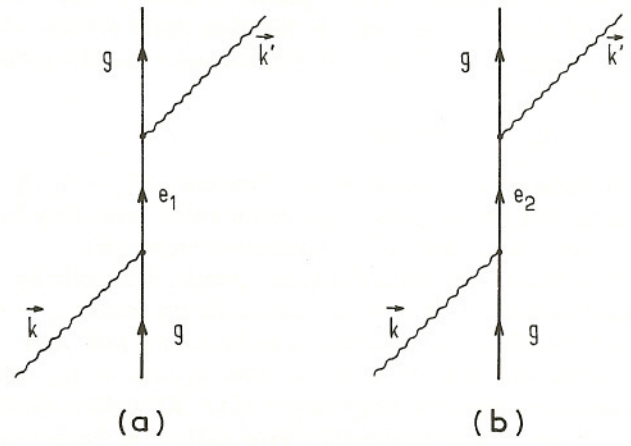

Fig. 2. Diagrammatic representation of the two scattering processes which contribute to the resonant scattering amplitude. The absorption of the incident photon $\boldsymbol{k}$ excites the atom either to e_1 (Fig. a) or to e_2 (Fig. b). The atom then returns to g by emission of the scattered photon $\boldsymbol{k}'$.

* Laboratoire associé au CNRS et à l'Université Pierre et Marie Curie.

on such an anisotropy. In order to interpret the variations of the fluorescence light when an external parameter, such as B, is varied, one needs to determine the corresponding variations of σ_{12} (and also of σ_{11} and σ_{22}). In several cases [3, 4], it is possible to establish a rate equation for σ_{12} having the following form.

$$\dot{\sigma}_{12} = R - i\frac{E_1 - E_2}{\hbar}\sigma_{12} - \Gamma\sigma_{12} \tag{1}$$

and describing the various factors which determine the evolution of σ_{12} : optical excitation, which prepares σ_{12} at a rate R; free evolution in the field $\boldsymbol{B}$ at the Larmor frequency $(E_1 - E_2)/\hbar$; damping with a rate Γ due to spontaneous emission. Equation (1) allows a simple interpretation of various interesting effects which can be observed on the light emitted by an atom which has been prepared in a linear superposition of excited Zeeman sublevels.

Suppose first that the intensity of the exciting light beam is constant. R is then constant, and Equation (1) has a steady-state solution.

$$\sigma_{12} = \frac{\hbar R}{i(E_1 - E_2) + \hbar\Gamma} \tag{2}$$

which clearly exhibits resonant variations around the crossing point $E_1 - E_2$ in an interval of width $\hbar\Gamma$. This provides a quantitative interpretation of the Hanle effect and of the Franken effect.

One can also use a modulated excitation:

$$R = R_0\, e^{-i\Omega t} \tag{3}$$

Equation (1) then admits a solution of the form:

$$\sigma_{12}(t) = \frac{\hbar R_0}{i(E_1 - E_2 - \hbar\Omega) + \hbar\Gamma}\, e^{-i\Omega t} \tag{4}$$

which shows that σ_{12} contains modulations at the same frequency Ω as the exciting light and which exhibit resonant variations when $E_1 - E_2$ is scanned around $\hbar\Omega$. Such resonant modulations of the fluorescence light have been observed by Corney and Series on cadmium atoms [5].

Another interesting situation is found when one uses a percussional excitation:

$$R = R_0\,\delta(t) \tag{5}$$

$\delta(t)$ being the delta fonction (more physically, one uses a pulse of exciting light, with a duration much smaller than $\hbar/|E_1 - E_2|$ and $1/\Gamma$). For $T > 0$, the solution of equation (1) reads

$$\sigma_{12}(t) = R_0\, e^{-i(E_1 - E_2)t/\hbar}\, e^{-\Gamma t} \tag{6}$$

Such damped oscillations at the frequency $(E_1 - E_2)/\hbar$ are nothing but the so-called " quantum beats" and they have been first observed in 1964 on cadmium atoms [6].

Note finally that, even if it is not prepared directly by the optical excitation ($R = 0$), σ_{12} can build up from $\sigma_{11} - \sigma_{22}$ under the effect of a resonant radiofrequency field $\boldsymbol{B}_1\, e^{-i\Omega t}$, perpendicular to $\boldsymbol{B}$. Modulations then appear in σ_{12} which are resonant when the frequency Ω of the RF field is close to $(E_1 - E_2)/\hbar$. The corresponding modulations at frequency Ω of the fluorescence light have been called " light beats" [7].

All the previous considerations can be easily extended to the case when there are several Zeeman sublevels $g_1, g_2 \ldots$ in the atomic ground state g. Similar equations of motion can be established [3, 4] for the atomic density matrix in g. Zeeman (or hyperfine) coherences can be introduced in g, either by the optical excitation itself, using for example a transverse or modulated optical pumping, or by applying a resonant radiofrequency (or microwave) field which drives a transition connecting two ground state sublevels belonging to the same hyperfine level (or to two different hyperfine levels). Resonances similar to those described above can be observed in atomic ground states by monitoring the absorbed light or the reemitted light. Because relaxation times are much longer in the ground state g than in the excited state e, these resonances are much narrower.

In this paper, we review a few of these narrow resonances associated with linear superpositions of atomic ground state sublevels. They were first observed, using an optical detection of the atomic internal state. We also describe new applications of these narrow resonances in the field of laser cooling and trapping by showing how the motion of the atomic center of mass can be influenced and controlled by preparing the atom in a linear superposition of ground state sublevels.

After a brief reminder on optical pumping and light shifts, we describe in section 2 a few applications of level crossing resonances in atomic ground states. We show how they can be used to detect very weak magnetic fields (less than 10^{-9} Gauss), or to change an atomic trajectory. We then consider in section 3 the case when Zeeman coherences in g are introduced by a modulated transverse pumping or by a resonant radiofrequency field. We also interpret in this way the so-called "velocity selective resonances" for an atom moving in a standing wave. Finally we discuss in section 4 the quenching of absorption of light by coherent population trapping. After a brief description of the first observation of this effect on sodium atoms excited by a multimode laser beam, we show how velocity selective coherent population trapping can be used to cool atoms below the limit corresponding to the recoil kinetic energy of an atom absorbing or emitting a single photon.

2. Level crossing resonances in atomic ground states

2.1. *Optical pumping and light shifts*

The principle of optical pumping is well known [8] and can be simply explained for an atomic transition connecting a ground state with an angular momentum $J_g = 1/2$ to an excited state with angular momentum $J_e = 1/2$ (Fig. 3). Suppose that a right circularly polarized (σ^+) light beam propagating along the z – axis excites resonantly such a transition for atoms contained in a cell (Fig. 3a). The frequency ω_L of the light is equal to the atomic frequency ω_A. Let $|g_{\pm 1/2}\rangle_z$ and $|e_{\pm 1/2}\rangle_z$ be the eigenstates of J_z in g and e, respectively. Because of the polarization selection rules, the σ^+ resonant light can excite only the $\Delta m = 1$ transition $|g_{-1/2}\rangle_z \leftrightarrow |e_{+1/2}\rangle_z$. Atoms initially in $|g_{-1/2}\rangle_z$ can thus be excited in $|e_{+1/2}\rangle_z$ from where they can fall back, either in $|g_{-1/2}\rangle_z$ by spontaneous emission of a σ^+ photon, in which case the same cycle can be repeated, or in $|g_{+1/2}\rangle_z$ by spontaneous emission of a π photon, in which case they remain trapped in $|g_{+1/2}\rangle_z$ because no σ^+ transition starts from $|g_{+1/2}\rangle_z$ (Fig. 3b). Such optical pumping cycles $|g_{-1/2}\rangle_z \rightarrow |e_{+1/2}\rangle_z \rightarrow |g_{+1/2}\rangle_z$ are a simple and efficient

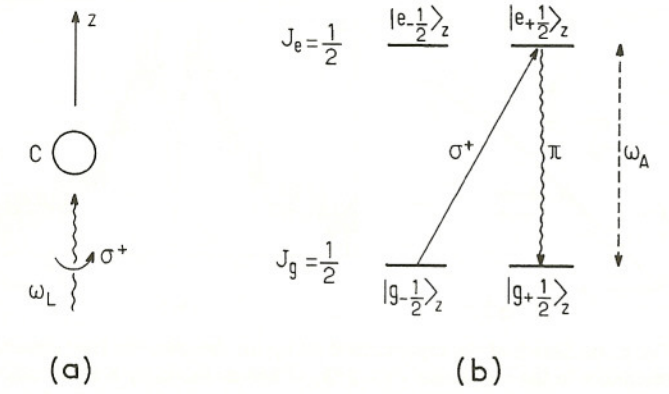

Fig. 3. Principle of optical pumping. (a) A σ^+-polarized resonant light beam, propagating along the z – axis, excites atoms contained in a cell. (b) Zeeman sublevels of the $J_g = 1/2 \leftrightarrow J_e = 1/2$ atomic transition. The upward arrow represents the transition which is excited by the σ^+ light. The downward wavy arrow represents the subsequent spontaneous emission of π-polarized light.

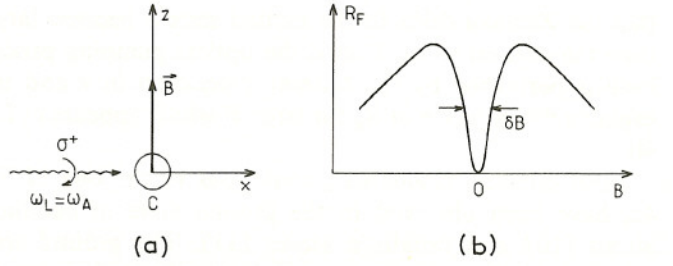

Fig. 4. (a) Relative disposition of the σ^+ optical pumping beam and of the static magnetic field in a transverse optical pumping experiment. (b) Sketch of the variations of the steady state fluorescence rate R_F versus B_0 for a $J_g = 1/2 \leftrightarrow J_e = 1/2$ transition.

way to polarize the atomic sample, i.e. to prepare atoms in a spin state oriented along the direction of the σ^+ pumping beam.

If the light beam is detuned from resonance, i.e. if $\omega_L \neq \omega_A$, one can show that the non resonant optical excitation produces an energy shift of the ground state sublevels [3, 4, 9] which are called light shifts or ac-Stark shifts. The magnitude of such light shifts is proportional to the light intensity and inversely proportional to the detuning $\delta = \omega_L - \omega_A$ (in the limit when the Rabi frequency Ω_1 describing the light-atom interaction is small compared to $|\delta|$). Because of the polarization selection rules, light shifts depend on the polarization of the exciting light and vary from one Zeeman sublevel to another. For example, in the case of Fig. 3, the σ^+ incident light shifts only the $|g_{-1/2}\rangle_z$ sublevel (if $\omega_L \neq \omega_A$). In the absence of external static magnetic field, the two Zeeman sublevels which are degenerate when the light beam is off, become separated by an amount equal to the light shift of level $|g_{-1/2}\rangle_z$ when the light beam is on. This shows that a σ^+ non-resonant light beam produces in a $J_g = 1/2$ atomic ground state energy splittings which are equivalent to those which would be produced by a fictitious magnetic field $\boldsymbol{B}_f$ parallel to the direction of propagation of the light beam [9]. Such a result will be useful for the interpretation of a recent experiment described in a subsequent section (§ 3.2).

2.2. *Transverse optical pumping*

We suppose now that a static magnetic field $\boldsymbol{B}_0$ is applied along the z-axis and that the σ^+ resonant pumping beam propagates along the x-axis, i.e. in a direction transverse with respect to the quantization axis defined by $\boldsymbol{B}_0$ (Fig. 4a). We have then a competition between two processes with different symmetries.

(i) Optical pumping which tends to prepare atoms in a spin state oriented along the direction of the σ^+ resonant light beam, i.e. in the eigenstate $|g_{+1/2}\rangle_x$ of J_x, which is a linear superposition of the eigenstates $|g_{+1/2}\rangle_z$ and $|g_{-1/2}\rangle_z$ of J_z.

$$|g_{+1/2}\rangle_x = \frac{1}{\sqrt{2}}\left[|g_{+1/2}\rangle_z + |g_{-1/2}\rangle_z\right] \tag{7}$$

(ii) Coupling with the static field B_0, which introduces an energy splitting $\hbar\Omega_L$ between $|g_{+1/2}\rangle_z$ and $|g_{-1/2}\rangle_z$, proportional to B_0, giving rise to a Larmor precession of the spins around the z – axis at the Larmor frequency Ω_L.

If $\boldsymbol{B}_0 = \boldsymbol{0}$, $|g_{+1/2}\rangle_z$ and $|g_{-1/2}\rangle_z$ are degenerate as well as their linear combinations $|g_{+1/2}\rangle_x$ and $|g_{-1/2}\rangle_x$. Atoms are optically pumped by the σ^+ resonant light beam into states $|g_{+1/2}\rangle_x$ which are stationary and do not evolve by Larmor precession. Since no σ^+ transition (with respect to the x-axis) starts from $|g_{+1/2}\rangle_x$ (see Fig. 3b, where z is replaced by x), an atom optically pumped in $|g_{+1/2}\rangle_x$ cannot also absorb light. For $\boldsymbol{B}_0 = \boldsymbol{0}$, the state $|g_{+1/2}\rangle_x$ is thus a perfect trap for atoms which cannot leave this state, either by photon absorption, or by Larmor precession. Such states are also called " dark states" . One understands in this way why the steady-state fluorescence rate R_F vanishes for $B_0 = 0$ (see Fig. 4b): after a transient regime, lasting a time on the order of the optical pumping time τ_P, all atoms are optically pumped into the dark state $|g_{+1/2}\rangle_x$. If relaxation processes (characterized by a relaxation time τ_R) are present, collisional transfers can occur between $|g_{+1/2}\rangle_x$ and $|g_{-1/2}\rangle_x$, and R_F no longer vanishes for $\Delta = 0$.

When B_0 is increased, the state $|g_{+1/2}\rangle_x$ into which atoms are optically pumped is coupled by the Zeeman Hamiltonian describing the interaction with $\boldsymbol{B}_0$ to $|g_{-1/2}\rangle_x$. In other words, the Larmor precession in the plane perpendicular to $\boldsymbol{B}_0$ transforms $|g_{+1/2}\rangle_x$ into a linear superposition of $|g_{+1/2}\rangle_x$ and $|g_{-1/2}\rangle_x$. Since σ^+ transitions (with respect to the x-axis) can start from $|g_{-1/2}\rangle_x$ (see Fig. 3b, where z now is replaced by x), an atom in such a linear superposition can absorb light and this explains why the fluorescence reappears when B_0 is increased (see Fig. 4b). In fact, the coherent Larmor precession is interrupted by optical pumping and relaxation processes which occur at a rate $\tau_g^{-1} \simeq \tau_P^{-1} + \tau_R^{-1}$, where τ_g is the total damping time in the ground state. If $\Omega_L \tau_g \ll 1$, the spin rotates by a very small angle during the damping time τ_g, so that the steady-state fluorescence rate R_F remains very small. If on the other hand $\Omega_L \tau_g \gg 1$, the rotation angle is very large and the spin orientation is equally distributed in the plane perpendicular to $\boldsymbol{B}_0$ leading to a plateau for R_F. The critical value δB_0 of the field giving the width of the narrow dip of Fig. 4b, corresponds to a Larmor frequency $\delta\Omega_L = \gamma \delta B_0$ (γ being the gyromagnetic ratio) such that $\delta\Omega_L \tau_g \sim 1$. We thus have

$$\delta B_0 \sim \frac{1}{\gamma \tau_g}, \tag{8}$$

the optimal signal to noise ratio being obtained when τ_P and τ_R are of the same order. Finally, when B_0 is so large

that the Zeeman shifts in the excited state e become larger than the natural width Γ of e, the optical pumping process itself is perturbed by the Larmor precession in e and this explains the decrease of R_F for large B which appears in Fig. 4b.

Level crossing resonances, analogous to the one of Fig. 4b, have been observed in the ground state of cadmium atoms [10] and rubidium atoms [11]. The ground state paramagnetism in the first case is due to the nuclear spin of cadmium, and to the electron spin in the second case, leading to higher values of Ω_L, of the order of 10^6 Hz per Gauss. In paraffin coated cells, the damping time τ_g of rubidium atoms in g can reach values of the order of 1 sec, so that δB_0 is, according to Eq. (8), very small, on the order of 10^{-6} Gauss. Fig. 5a gives an example of level crossing resonance observed in the ground state of ^{87}Rb [11]. A modulation of the amplitude of $\boldsymbol{B}_0$ allows one to get dispersion shaped curves more convenient than the absorption shaped curve of Fig. 4b for measuring the center of the resonance. The signal to noise ratio is very high, on the order of 10^4 so that very small variations of B_0 can be easily detected. Fig. 5b shows the response of the signal to applied square variations of B_0, with an amplitude of 2.10^{-9} Gauss. One sees that one can detect variations of the static field on the order of 5.10^{-10} Gauss. Such a magnetometer has been used to detect the magnetostatic field produced at a macroscopic distance ($\sim$6 cm) by a gaseous sample of ^{3}He atoms, whose nuclei were oriented by optical pumping [12].

2.3. *Mechanical detection of the level crossing resonance*

The analysis of the previous section shows that the amount of light absorbed by an atom in a transverse optical pumping experiment varies in a resonant way when the magnetic field B is scanned around 0. The momentum absorbed by the atom, and consequently the radiation pressure force exerted by the pumping beam, should therefore exhibit similar resonant variations. Level crossing resonances in atomic ground states can thus be also detected by a modification of atomic trajectories.

An experiment of this type has been performed on metastable helium atoms [13]. Fig. 6a gives a sketch of the experimental set up. A beam of helium atoms in the $2\,^3S_1$ metastable state propagates along the y-axis. A σ^+ resonant laser beam, propagating along the x-axis excites the transition $2\,^3S_1 \leftrightarrow 2\,^3P_1$ at 1.08 μm. The arguments presented above for a $J_g = 1/2 \leftrightarrow J_e = 1/2$ transition remain valid for the $J_g = 1 \leftrightarrow J_e = 1$ transition considered here. When $\boldsymbol{B}_0 = \boldsymbol{0}$, after a transient regime, all atoms are optically pumped in the dark state $|g_{+1}\rangle_x$ and the absorption stops. The deflection of the atomic trajectory is small. When $\boldsymbol{B}_0$ is increased, the Larmor precession in the plane perpendicular to $\boldsymbol{B}_0$ couples $|g_{+1}\rangle_x$ to $|g_0\rangle_x$ and $|g_{-1}\rangle_x$, which can absorb light. The corresponding increase of radiation pressure gives rise to a larger deflection. By putting along the y-axis, and slightly off axis in the horizontal plane, a detector which records the metastable helium atoms, one gets a signal which is sensitive to the deflection of the atoms and whose variations with B_0 are represented in Fig. 6b. The narrow dip of Fig. 6b provides a mechanical detection of the level crossing resonance in the metastable state of helium. It has been very useful for adjusting in situ the static magnetic field to zero in subrecoil laser cooling experiments. The number of metastable atoms in the beam is rather small and an optical detection of the resonance by observation of the fluorescence light emitted on the $2\,^3P_1 \leftrightarrow 2\,^3S_1$ transition is difficult. On the other hand, detection of metastable atoms which carry a large internal energy is very sensitive.

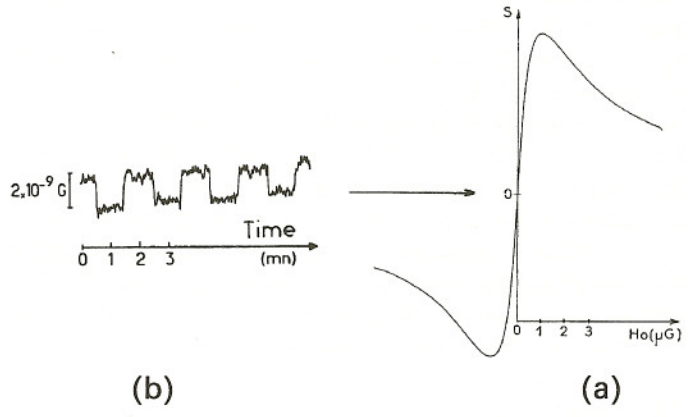

Fig. 5. (a) Example of zero field level crossing resonance observed in the ground state of ^{87}Rb atoms. (b) Response of the signal S to applied square variations of the static magnetic field. The signal to noise ratio allows one to detect variations of B_0 as small as $5\ 10^{-10}$ Gauss.

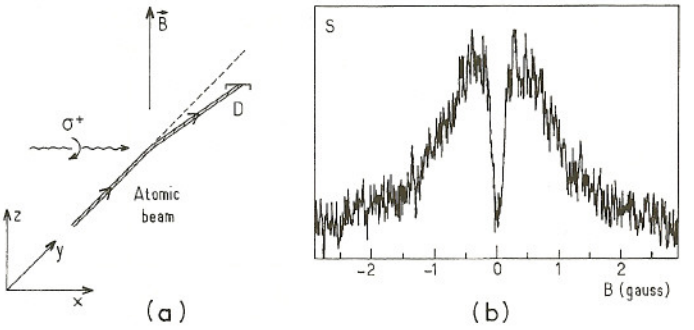

Fig. 6. (a) Sketch of the experimental set up for detecting the level crossing resonance in the metastable state $2\,^3S_1$ of helium atoms by a modification of the atomic trajectories. (b) Signal S recorded by the detector D when B_0 is scanned. The narrow dip around B_0 corresponds to the level crossing resonance.

3. Ground state Zeeman coherences induced by a modulated transverse pumping or a resonant RF field

3.1. *A few early experiments*

We consider first transverse pumping experiments with modulated light. The experiment scheme is the same as in Fig. 4a. The static field $\boldsymbol{B}_0$ is now large and we have $\Omega_L \tau_g \gg 1$, so that the spin orientation introduced along Ox is completely smeared out by the Larmor precession around $\boldsymbol{B}_0$. Suppose that the light intensity, instead of being constant, is modulated at the frequency Ω and consider the simple case where it consists of pulses equally spaced in time, with a separation $2\pi/\Omega$ between two successive pulses. Just after a pulse, a spin is optically pumped along the x-axis. When the next pulse arrives, such a spin has rotated by an angle $\theta = \Omega_L 2\pi/\Omega$. If $\Omega_L = \Omega$, $\theta = 2\pi$ and the spin is again oriented along the $x-$axis, so that it will not be perturbed by the new pulse since it cannot absorb it. Furthermore, the new pulse will optically pump new atoms whose spins are in phase with the previous ones, so that there will be cumulative effect of optical pumping: one gets a net spin orientation rotating at frequency Ω and whose amplitude and

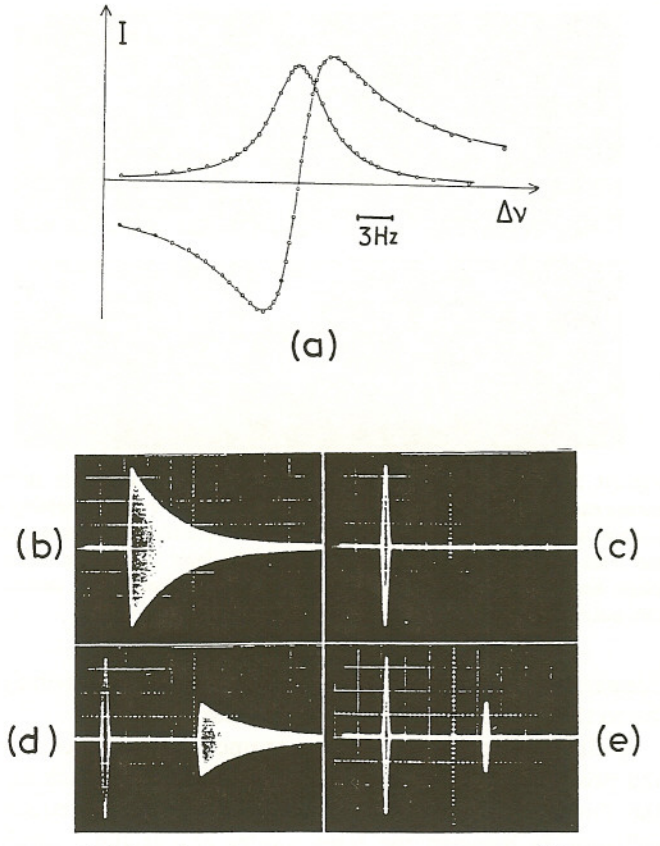

Fig. 7. Optical detection of NMR in the ground state of ^{199}Hg by the modulation of the absorption of a weak transverse probe beam (from [4]). In Fig (a), the RF field amplitude is constant and the field B_0 is scanned around the value corresponding to $\Omega_L = \Omega$. The two curves represent the components of the modulation of the absorption signal in phase and in quadrature with the RF field (lock-in detection). The four next figures (b, c, d, e) represent the modulations detected when the RF field amplitude is pulsed) Ω_L being equal to Ω. b: π/2pulse; c:π pulse; d: sequence of one π and one $\pi/2$ pulses; e: sequence of two pulses. The decay of the signal of Fig. 7b gives the T_2-relaxation time. The decay of the signal from one pulse to the next one in Figs 7d and 7e gives the T_1-relaxation time.

phase will vary in a resonant way when Ω is scanned around Ω_L (or when, Ω being fixed, B_0 is scanned around the value corresponding to $\Omega_L = \Omega$). Such resonant modulations of the spin orientation in g, which have been first observed on sodium atoms [14], are the equivalent for atomic ground states of the resonances described by equations (3) and (4) for atomic excited states.

We describe now another experiment which can be considered as the extension to atomic ground states of the light-beat experiment of George Series. A longitudinal σ^+ polarized beam (parallel to $\boldsymbol{B}_0$) optically pumps the atoms in the state $|g_{+1/2}\rangle_z$ (see Fig. 3). Under the effect of a resonant RF field $\boldsymbol{B}_1 \cos \Omega t$, perpendicular to $\boldsymbol{B}_0$, such a state is transformed into a linear superposition of $|g_{+1/2}\rangle_z$ and $|g_{-1/2}\rangle_z$, which gives rise to a transverse spin orientation rotating at frequency Ω in the plane perpendicular to $\boldsymbol{B}_0$, with an amplitude and a phase varying in a resonant way around $\Omega_L = \Omega$. If now we apply a weak probe σ^+-polarized beam along the x-axis, the absorption of such a probe beam will be modulated at frequency Ω by the rotating spin orientation: the σ^+ probe beam is not absorbed when the spins are in the $|g_{+1/2}\rangle_x$ state whereas it is absorbed when the spins are in the $|g_{-1/2}\rangle_x$ state. As in usual magnetic resonance experiments where one detects the voltage induced in a coil by the rotating magnetic moments, the detection signal is here proportional to the transverse spin orientation. But it is now an optical signal, much more sensitive than a radio-frequency one. Figure 7 gives for example detection signals of the nuclear magnetic resonance in the ground state of ^{199}Hg, which has a purely nuclear paramagnetism. Such signals are obtained by monitoring the modulation of the absorption of a weak transverse beam. Although there are only about 10^{12} oriented nuclei per cm^3 in a cell of about 10 cm^3, the signal to noise ratio is quite good. With such a low density, an usual radio-frequency detection of NMR would be rather difficult.

3.2. *Velocity selective resonances*

We describe now a recent laser cooling experiment [15] and show how velocity selective resonances observed in this experiment can be interpreted in terms of a modulated transverse optical pumping.

Figure 8 gives a sketch of the experimental set up. A σ^+-polarized standing wave, $E_0 \sin kx \sin \omega_L t$, propagates along the x-axis. It is crossed by an atomic beam propagating along the z-axis. Because of the non perfect collimation of the atomic beam, there is a certain velocity spread along the x-axis. A static magnetic field $\boldsymbol{B}_0$ is applied along the z-axis. The measured signal is the number of atoms detected by a hot wire put far away along the z-axis. Such a signal is proportional to the velocity distribution of atoms along the x-axis.

Consider an atom moving along the x-axis with a velocity v_x. Because the intensity of the standing wave is spatially modulated with a period $\lambda/2 = \pi/k$, such an atom "sees" a σ^+ light whose intensity $I(t)$ is modulated in time: $I(t) = I_0 \cos \Omega t$ where

$$\Omega = 2\pi \frac{v_x}{\lambda/2} = 2kv_x \tag{9}$$

Let $\Omega_L = g\mu_B B_0/\hbar$ be the Larmor frequency at which the atoms precess in the static field B_0(g is the g-factor, μ_B the Bohr magneton). According to the results of the previous section 3.1, the modulated transverse optical pumping experienced by the moving atom gives rise to a modulated transverse magnetization $M_x(t) = M_0 \cos(\Omega t - \varphi)$ whose amplitude M_0 and phase φ vary in a resonant way around $\Omega_L = \Omega$. If the laser frequency Ω_L is slightly different from

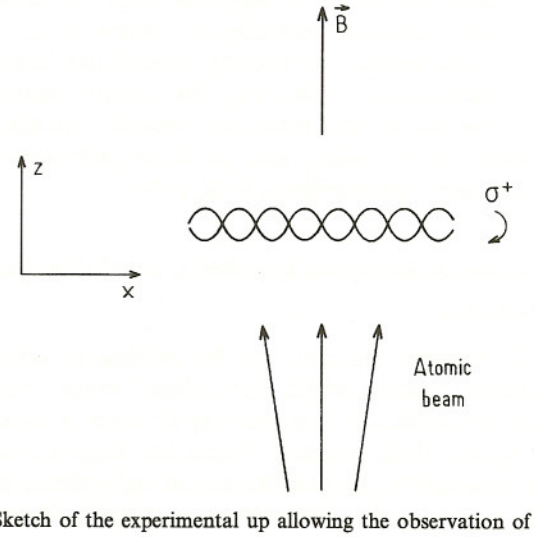

Fig. 8. Sketch of the experimental up allowing the observation of velocity selective resonances.

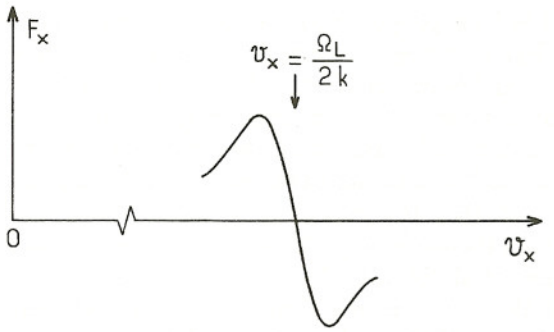

Fig. 9. Variations with v_x of the force F_x experienced by an atom moving with velocity v_x along the standing wave. Around the value $v_x = \Omega_L/2k$, these variations have a dispersion shape.

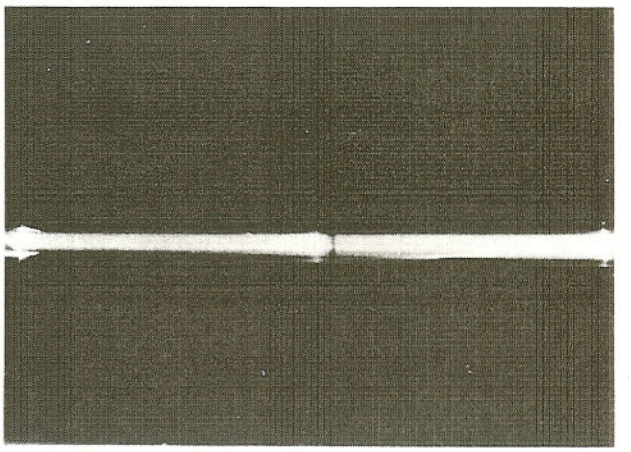

Fig. 10. Spatial variations of the fluorescence light emitted by sodium atoms excited by a multimode resonant laser beam. The cell containing the sodium atoms is put in a magnetic field gradient parallel to the direction of the laser beam. At certain positions along the laser beam, one observes black lines corresponding to a quenching of absorption which occurs at this position (from Ref. 16).

the atomic frequency ω_A, there are also light shifts. As shown at the end of section 2.1, the effect of these light shifts is equivalent to the effect of a fictitious magnetic field parallel to the direction of propagation of the σ^+-polarized beam and proportional to the light intensity. It follows that the moving atom not only experiences a modulated transverse pumping but is also submitted to a modulated fictitious field $B_f(t) = B_1 \cos \Omega t$ parallel to the x-axis. Such a modulated field can exchange energy with the modulated transverse magnetization if $\overline{M_x(t) dB_f(t)} \neq 0$, the average being taken over one oscillation period. Evaluation of such an energy exchange gives some physical insight into the force F_x experienced by the atom moving with velocity v_x along the standing wave.

Suppose first that $v_x = \Omega_L/2k$, so that, according to (9), $\Omega_L = \Omega$. $M_x(t)$ is then in phase with $I(t) = I_0 \cos \Omega t$, as well as $B_f(t)$. It follows that $M_x(t)$ and $B_f(t)$ oscillate in phase, so that $\overline{M_x(t) dB_f(t)} = 0$. There is no exchange of energy and $F_x = 0$. If v_x is slightly different from $\Omega_L/2k$, Ω is no longer equal to Ω_L. $M_x(t)$ has now a component in quadrature with $I(t)$, whereas $B_f(t)$ is still in phase with $I(t)$. $M_x(t)$ and $B_f(t)$ are thus no longer in phase, so that $\overline{M_x(t) dB_f(t)} \neq 0$. We have now an exchange of energy between the atom and the field and F_x is no longer equal to zero. All these results are summarized in Fig. 9 which gives the variations with v_x of the force F_x experienced by the atom. These variations have a dispersive shape around $v_x = \Omega_L/2k$. For a certain sign of the detuning $\delta = \omega_L - \omega_A$, the slope of the curve at $v_x = \Omega_L/2k$ is negative, which means that such an equilibrium point is stable. Atomic velocities are locked at $v_x = \Omega_L/2k$ and there is, in addition, a cooling around this value of v_x. One can understand in this way the narrow peaks which can be observed in the transverse velocity profile of the transmitted atomic beam, and which appear around non zero values of v_x, proportional to B_0 [15].

4. Quenching of absorption by coherent population trapping

4.1. *Black lines*

In 1976, Adriano Gozzini and his colleagues observed a very interesting effect which they called " black lines" [16]. Consider a multimode laser passing through a sodium cell in a magnetic field gradient. When the laser frequency is close to resonance, the fluorescence of the sodium vapor is excited and the path of the beam is bright. However, at certain positions along the laser beam, the fluorescence disappears, which gives rise to a narrow black line perpendicular to the direction of the laser beam (see Fig. 10).

A closer examination of the parameters which determine the position of the black line reveals that the quenching of the fluorescence occurs at the places where the frequency splitting $\delta\nu$ between the laser modes equals the hyperfine frequency splitting between two Zeeman sublevels $|F_1, m_1\rangle$ and $|F_2, m_2\rangle$ belonging to the two ground hyperfine levels F_1 and F_2 of sodium atoms. Because of the magnetic field gradient, the Zeeman shifts of $|F_1, m_1\rangle$ and $|F_2, m_2\rangle$ are position dependent and this explains why the resonance condition is fulfilled only at certain positions. Consider the simplified model of Fig. 11 where a three-level atom with two Zeeman sublevels g_1 and g_2 and a single excited sublevel e_0 is excited by two laser fields with frequencies ω_{L1} and ω_{L2}, exciting the transitions $g_1 \leftrightarrow e_0$ and $g_2 \leftrightarrow e_0$, respectively. Let $\hbar\Delta$ be the detuning from resonance for the stimulated Raman process consisting of the absorption of one photon ω_{L1} and the stimulated emission of one ω_{L2} photon, the atom going from g_1 to g_2 (Fig. 11). The experimental results of Ref. 16 show that the fluorescence disappears when $\Delta = 0$.

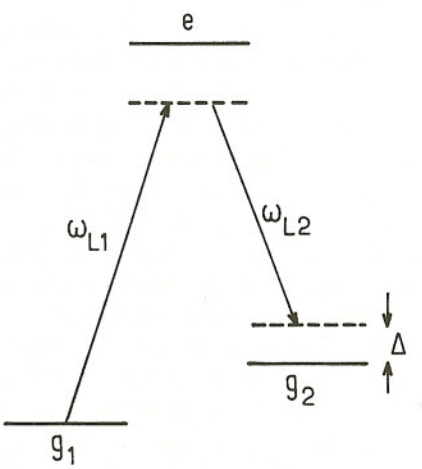

Fig. 11. Three-level atom $\{g_1, g_2, g_0\}$ excited by two laser fields with frequencies ω_{L1} and ω_{L2} exciting the transitions $g_1 \leftrightarrow e_0$ and $g_2 \leftrightarrow e_0$, respectively. $\hbar\Delta$ is the detuning from resonance for the stimulated Raman process induced between g_1 and g_2 by the two laser fields ω_{L1} and ω_{L2}.

Soon after the discovery of black lines, a theoretical analysis was performed [17] consisting in solving the optical Bloch equations for the density matrix σ of the simplified three-level model of Fig. 11. For the variations with Δ of the fluorescence rate $R_F = \Gamma\langle e_0|\sigma|e_0\rangle$ (Γ being the spontaneous emission rate from e_0), one finds the results sketched in Fig. 12: R_F strictly vanishes for $\Delta = 0$. The narrow dip of Fig. 12 has a width Γ' determined by the damping rates of the ground state which are much smaller than the damping rate Γ of the excited state e_0, responsible for the slow decrease of R_F appearing in Fig. 12 for large values of Δ. Another important result of such a calculation is that the vanishing of $\langle e_0|\sigma|e_0\rangle$ for $\Delta = 0$ is accompanied by the appearance of a "hyperfine coherence" $\langle g_1|\sigma|g_2\rangle$ whose modulus is equal to 1 for $\Delta = 0$. In other words, the black line is associated with a trapping of atoms in a linear superposition of the ground state sublevels g_1 and g_2, such that the two absorption amplitudes from g_1 to e_0 and from g_2 to e_0 interfere destructively.

The dressed-atom approach is also very useful for analyzing such an effect [18]. The uncoupled states of the atom + laser photons system are grouped into well separated three-dimensional manifolds of closely spaced states.

$$\{|e_0, N_1, N_2\rangle, \quad |g_1, N_1 + 1, N_2\rangle, \quad |g_2, N_1, N_2 + 1\rangle\} \tag{10}$$

where N_1 and N_2 are the number of ω_{L1} photons and ω_{L2} photons, respectively. The energy splitting between $|g_1, N_1 + 1, N_2\rangle$ and $|g_2, N_1, N_2 + 1\rangle$ is nothing but

$$Eg_1 - Eg_2 + \hbar(\omega_{L1} - \omega_{L2}) = \hbar\Delta \tag{11}$$

which means that, for $\Delta = 0$, the two uncoupled states $|g_1, N_1 + 1, N_2\rangle$ and $|g_2, N_1, N_2 + 1\rangle$ are degenerate. Because the atom in $|g_1\rangle$ can absorb one ω_{L1} photon and go to $|e_0\rangle$, the two states $|g_1, N_1 + 1, N_2\rangle$ and $|e_0, N_1, N_2\rangle$ are coupled by the atom-laser interaction Hamiltonian V_{AL}. A similar result holds for $|g_2, N_1, N_2 + 1\rangle$ and $|e_0, N_1, N_2\rangle$. There is therefore a linear superposition of $|g_1, N_1 + 1, N_2\rangle$ and $|g_2, N_1, N_2 + 1\rangle$ which is not coupled to the excited state because of a destructive quantum interference between the two amplitudes $|g_1, N_1 + 1, N_2\rangle \rightarrow |e_0, N_1, N_2\rangle$ and $|g_2, N_1, N_2 + 1\rangle \rightarrow |e_0, N_1, N_2\rangle$. Furthermore, this linear superposition is also stationary when $\Delta = 0$, because the two states $|g_1, N_1 + 1, N_2\rangle$ and $|g_2, N_1, N_2 + 1\rangle$ are then degenerate. This shows that there is a dark state when $\Delta = 0$, which becomes less and less dark when Δ increases. The narrow dip of Fig. 12 can thus be interpreted as a level crossing resonance in the dressed atom energy diagram. This establishes a connection between coherent population trapping and the Hanle effect discussed in sections 1 and 2 and explains why the curves of Figures 4b and 12 are so similar.

4.2. *Subrecoil laser cooling by velocity selective coherent population trapping (VSCPT)*

The quenching of absorption by quantum interference effects has recently found interesting applications in the field of laser cooling. By introducing a velocity dependence in coherent population trapping, it has been possible to cool atoms below the so called recoil limit corresponding to the kinetic energy of an atom initially at rest and absorbing or emitting a single photon.

The basic idea consists in making the detuning Δ from resonance for the stimulated Raman process of Fig. 11 proportional to the atomic velocity v. In a one-dimensional laser cooling experiment along the z-axis, this is achieved by taking the two laser beams counterpropagating along this axis and by adjusting ω_{L1} and ω_{L2} so that

$$\hbar(\omega_{L1} - \omega_{L2}) = Eg_2 - Eg_1 \tag{12}$$

If the atomic velocity v along the $z-$ axis is equal to zero, there is no Doppler shift and equation (12) is equivalent to $\Delta = 0$ [see eq. (11)]. If $v \neq 0$, the two Doppler shifts $k_1 v$ and $-k_2 v$ of the two counterpropagating waves are nearly opposite since $k_1 \simeq k_2 = k$. It follows that $\omega_{L1} - \omega_{L2}$ has to be replaced by $\omega_{L1} + kv - (\omega_{L2} - kv) = \omega_{L1} - \omega_{L2} + 2kv$, which shows that we have now a detuning $\Delta = 2kv$ which is proportional to v. The variations of the fluorescence rate R_F with the atomic velocity v are thus similar to those of Fig. 12, since varying v is equivalent to varying the detuning Δ from Raman resonance. Consider then an atom with $v = 0$. For such an atom, $\Delta = 0$ and the absorption of light is quenched. Consequently, there is no spontaneous reemission and no associated random recoil. One protects in this way ultracold atoms (with $v \simeq 0$) from the "bad" effects of the light. On the other hand, atoms with $v \neq 0$ can absorb and reemit light. In such an absorption-spontaneous emission cycle, their velocities change in a random way and the corresponding random walk in v-space can transfer atoms from the $v \neq 0$ absorbing states into the $v \simeq 0$ dark states where they remain trapped and accumulate (see Fig. 13). This reminds us of what happens in a Kundt's tube where sand grains vibrate in an acoustic standing wave and accumulate

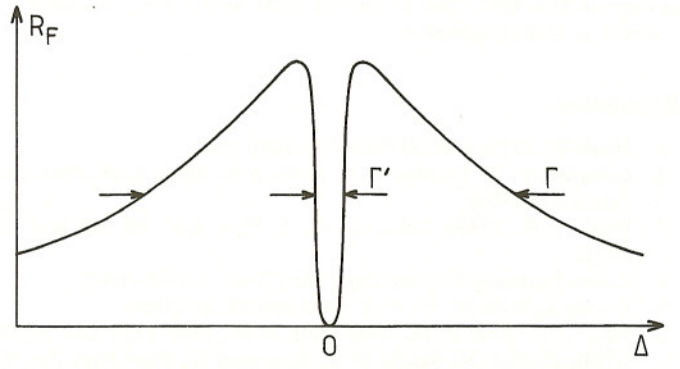

Fig. 12. Sketch of the variations with the detuning Δ from Raman resonance of the calculated fluorescence rate R_F for the three-level model of Fig. 11. R_F strictly vanishes for $\Delta = 0$. Γ' and Γ are related to the damping rates in the ground state and the excited state, respectively.

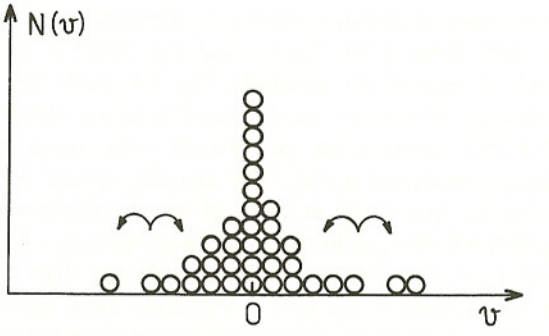

Fig. 13. Principle of laser cooling by velocity selective coherent population trapping. Atoms with $v = 0$ do not absorb light and do not recoil. Atoms with $v \neq 0$ absorb and reemit light. The corresponding random recoil can lead them near $v = 0$ where they remain trapped and pile up.

at the nodes of this wave where they no longer move. Note however that the random walk takes place in velocity space for the situation considered in Fig. 13, whereas it takes place in position space in a Kundt's tube.

Such a cooling mechanism has been demonstrated with metastable helium atoms [19]. The two lower states g_1 and g_2 are the $M = -1$ and $M = +1$ Zeeman sublevels of the $2\,^3S_1$ metastable state, e_0 is the $M = 0$ Zeeman sublevel of the excited $2\,^3P_1$ state. The two counterpropagating laser waves have the same frequency $\omega_{L1} = \omega_{L2} = \omega_L$ and have opposite circular polarizations. There is no external magnetic field so that $Eg_2 = Eg_1$ and condition (12) is fulfilled. A more quantitative analysis of the cooling process [20] shows that atoms are cooled into non-coupled states

$$|\psi_{NC}\rangle = c_1\,|g_1, p - \hbar k\rangle + c_2\,|g_2, p + \hbar k\rangle \qquad (13)$$

which are linear superpositions of two states which differ not only by the internal state (g_1 or g_2) but also by their momentum along the z-axis ($p - \hbar k$ or $p + \hbar k$). The coefficients c_1 and c_2 depend on the amplitudes of the two laser waves and on the Clebsch-Gordan coefficients of the two transitions $g_1 \leftrightarrow e_0$ and $g_2 \leftrightarrow e_0$. After an interaction time Θ, the momentum p which characterizes the states (13) into which atoms are cooled is distributed around $p = 0$ in an interval δp which decreases indefinitely when Θ increases: one finds that δp varies as $\Theta^{-1/2}$. If one defines a temperature T by the relation $k_B\,T/2 = \delta p^2/2M$, such a result shows that there is in principle no lower limit to the temperature T which can be achieved by VSCPT.

Two important theoretical developments have recently extended the applicability of VSCPT. First, it has been shown [21] that it is possible to extend VSCPT to two and three dimensions for a $J_g = 1 \leftrightarrow J_e = 1$ transition. One finds in such a case that the dark state into which atoms are cooled is described by the same vector field as the laser field. More precisely, if the laser field is formed by a linear superposition of N plane waves with wave vectors $\boldsymbol{k}_i (i = 1, 2, \ldots N)$ having the same modulus k, one finds that atoms are pumped into a coherent superposition of N wave packets with mean momenta $\hbar\boldsymbol{k}_i$ and with a momentum spread δp which becomes smaller and smaller when the interaction time Θ increases. Secondly, it has been shown [22–24] that it is possible to improve VSCPT with a precooling associated with a friction force pushing atoms to $\boldsymbol{p} = \boldsymbol{0}$ in $\boldsymbol{p}$-space. This is important for the extension of VSCPT to two and three dimensions since a pure random walk, such as in Fig. 13, would then be less and less efficient for bringing the atoms near $\boldsymbol{p} = \boldsymbol{0}$.

Experimental demonstrations of subrecoil cooling at two [25] and three [26] dimensions by VSCPT have been recently obtained. For example, Fig. 14 shows the velocity distribution of one of the six wave packets obtained in a 3D-VSCPT experiment performed with three pairs of counterpropagating waves. The velocity spread δv, defined as being the half width at $1/\sqrt{e}$ of this distribution, is equal to $v_R/4.8$, where $v_R = \hbar k/M$ is the recoil velocity. This corresponds to a temperature T 22 times lower than the recoil limit T_R, defined by $k_B\,T_R/2 = \hbar^2 k^2/2M$. Since $\delta p = M\delta v = \hbar k/4.8$, the coherence length of the atomic wave packet $\xi = h/\delta p$, is about 5 times longer than the laser wavelength $\lambda_L = 2\pi/k$, i.e. on the order of 5 microns. Note finally that the six coherent wave packets forming the dark state into

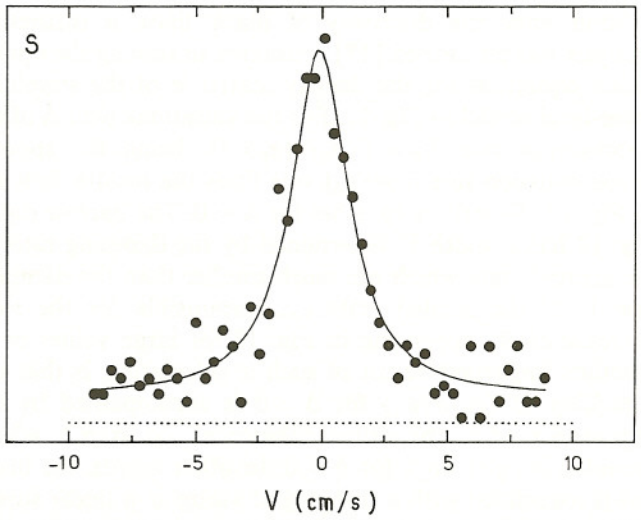

Fig. 14. Example of velocity distribution measured on one of the six coherent wave packets obtained in a 3D-VSCPT experiment. The dotted line gives the magnitude of the signal in the absence of VSCPT. The recoil velocity $v_R = \hbar k/M$ is equal to 9.2 cm/s for helium.

which atoms are laser cooled are separated in this experiment by a macroscopic distance, on the order of 1 cm.

5. Conclusion

I have reviewed in this paper several quantum interference effects which can be observed on the light absorbed or emitted by an atom which has been prepared in a linear superposition of two ground state or two excited state Zeeman sublevels. Such effects were discovered and studied several decades ago by physicists working in atomic physics, optical pumping and high resolution spectroscopy. I would like to dedicate this paper to three of these physicists, who have played a decisive role in the discovery and the investigation of these effects and who passed away recently : Wilhelm Hanle, Adriano Gozzini and George Series. I think that the best tribute that I could pay to their memory is to show, as I have tried to do here, that their ideas are still finding new important and fruitful applications in recent expanding research fields such as the laser manipulation of atoms.

Acknowledgements

I would like to thank Massimo Inguscio, Maria Allegrini and Antonio Sasso who invited me to present a lecture on the topics covered by this paper at the Twelth International Conference on Laser Spectroscopy, held in Capri in June 1995. Only a summary of the lecture was published in the proceedings of the Conference.

References

1. Hanle W., Z. Phys. **30**, 93 (1924); **35**, 346 (1926).
2. Colegrove F. D., Franken P. A., Lewis R. R., Sands R. H., Phys. Rev. Lett. **3**, 420 (1959).
3. Barrat J.-P., Cohen-Tannoudji C., J. Phys. Rad. **22**, 329 and 443 (1961).
4. Cohen-Tannoudji C., Ann. Phys. Paris **7**, 423 and 469 (1962).
5. Corney A., Series G. W., Proc. Phys. Soc. **83**, 207 (1964).
6. Dodd J. N., Kaul R. D., Warrington D. M., Proc. Phys. Soc. **84**, 176 (1964); Dodd J. N., Sandle W. J., Zisserman D., Proc. Phys. Soc. **92**, 497 (1967).
7. Dodd J. N., Fox W. N., Series G. W., Taylor M. J., Proc. Phys. Soc. **74**, 789 (1959); Dodd J. N., Series G. W., Proc. Roy. Soc., **A263**, 353 (1961); Dodd J. N., Series G. W., Taylor M. J., Proc. Roy. Soc., **A273**,

41 (1963); Kibble B. P., Series G. W., Proc. Roy. Soc., **A274**, 213 (1963).
8. Kastler A., J. Phys. Rad. **11**, 255 (1950).
9. Cohen-Tannoudji C., Dupont-Roc J., Phys. Rev. **A5**, 968 (1972).
10. Lehmann J.-C., Cohen-Tannoudji C., C. R. Acad. Sci. **258**, 4463 (1964).
11. Dupont-Roc J., Haroche S., Cohen-Tannoudji C., Phys. Lett. **28A**, 638 (1969).
12. Cohen-Tannoudji C., Dupont-Roc J., Haroche S., Laloë F., Phys. Rev. Lett. **22**, 758 (1969).
13. Kaiser R., Vansteenkiste N., Aspect A., Arimondo E., Cohen-Tannoudji C., Z. Phys. **D18**, 17 (1991).
14. Bell W. E., Bloom A. L., Phys. Rev. Lett. **6**, 280 (1961).
15. Chang S. Q., Sheevy B., van der Straten P., Metcalf H., Phys. Rev. Lett. **65**, 317 (1990).
16. Alzetta G., Gozzini A., Moi L., Orriols G., Il Nuovo Cimento **36B**, 5 (1976).
17. Arimondo E., Orriols G., Lett. Nuovo Cimento **17**, 333 (1976).
18. Dalibard J., Reynaud S., Cohen-Tannoudji C., in "Interaction of Radiation with Matter" , a volume in honour of Adriano Gozzini (Scuola Normale Superiore, Pisa, Italy, 1987), p. 29. See also Radmore P. M., Knight P. L., J. Phys. **B15**, 561 (1982).
19. Aspect A., Arimondo E., Kaiser R., Vansteenkiste N., Cohen-Tannoudji C., Phys. Rev. Lett. **61**, 826 (1988).
20. Aspect A., Arimondo E., Kaiser R., Vansteenkiste N., Cohen-Tannoudji C., J. Opt. Soc. Am. **B6**, 2112 (1989).
21. Ol'shanii M. A., Minogin V. G., in "Proceedings of Light Induced Kinetic Effects" (edited by L. Moi et al.) (Pisa, 1991); Ol'shanii M. A., Minogin V. G., Optics Commun. **89**, 393 (1992).
22. Shahriar M. S., Hemmer P. R., Prentiss M. G., Marte P., Mervis J., Katz D. P., Bigelow N. P., Cai T., Phys. Rev. **A48**, R4035 (1993).
23. Marte P., Dum R., Taïeb R., Zoller P., Shahriar M. S., Prentiss M., Phys. Rev. **A49**, 4826 (1994).
24. Weidmuller M., Esslinger T., Ol'shanii M. A., Hemmerich A., Hänsch T. W., Europhysics Lett. **27**, 109 (1994).
25. Lawall J., Bardou F., Saubamea B., Shimizu K., Leduc M., Aspect A., Cohen-Tannoudji C., Phys. Rev. Lett. **73**, 1915 (1994).
26. Lawall J., Kulin S., Saubamea B., Bigelow N. P., Leduc M., Cohen-Tannoudji C., Phys. Rev. Lett. **75**, 4194 (1995).